AUTO-STEREOSCOPIC RENDERING QUALITY ASSESSMENT DEPENDING ON POSITIONING ACCURACY OF IMAGE SENSORS IN MULTI-VIEW CAPTURE SYSTEMS

M. Ali-Bey, S. Moughamir and N. Manamanni

CReSTIC, Reims Champagne-Ardenne University, Moulin de la Housse, BP. 1039, 51687 Reims, France

Keywords: 3DTV, Multi-view capture, Auto-stereoscopy, 3D rendering quality assessment, Accurate positioning.

Abstract: Our interest in this paper concerns the quality assessment of the 3D rendering in a production process of auto-stereoscopic images using a multi-view camera with parallel and decentring configuration. The 3D rendering quality problem for such process is related to the coherence of the captured images of different viewpoints. This coherence depends, among others, on a rigorous respect of the shooting and rendering geometries. Assuming perfect rendering conditions, we are rather interested in the shooting geometry and image sensors positioning. This latter must be accurate enough to produce images that are quite coherent with each other and contribute fully to achieve a quality 3D content. The purpose of this paper is precisely to study the positioning accuracy of the different geometrical parameters of shooting based on a quality assessment of auto-stereoscopic rendering. We propose two different approaches for assessment of the 3D rendering quality. The first one is based on visual assessment tests of the 3D rendering quality by human observers. The second approach is based on the acquired scientific knowledge on human visual acuity. We present some simulation and experimental tests as well as the obtained results and their repercussion on the positioning accuracy of the shooting parameters.

1 INTRODUCTION

Nowadays, three-dimensional television (3DTV) knows a real revolution thanks to the technological headways in visualization, computer graphics and capture technologies. Depending on the technology adopted, the 3D visualization systems can be either stereoscopic or auto-stereoscopic. In stereoscopy, viewing glasses are required and different technologies are used to separate the left-eye and right-eye views: anaglyph or colour multiplexing (Sanders 2003), (Dubois, 2001), occultation and polarization multiplexing (Blach, 2005), time sequential presentation using active shuttering glasses (Meesters, 2004). Auto-stereoscopic displays do not need any special viewing glasses since they are direction-multiplexed devices equipped by parallax barriers or lenticular systems (Perlin, 2000), (Dodgson, 2002), (Meesters, 2004).

To supply these display devices by 3D contents, the more interesting and used methods are based on the synthesis of multiple viewpoint images from 2D-plus-depth data for stereoscopic display (Güdükbay, 2002) and auto-stereoscopic display (Müler, 2008). The transformation between viewing and capturing space with controlling perceived depth in stereoscopic case is described in (Graham, 2001). A generalized multi-view transformation model between viewing and capturing space with controlled distortion is proposed in (Prévoteau, 2010). A time varying concept of this architecture for dynamic scenes capture is reported in (Ali-Bey, 2010a), (Ali-Bey, 2010b).

In the present paper, we are interested in positioning accuracy of image sensors in such a multi-view camera. The purpose is to determine the positioning accuracy of different shooting parameters ensuring a satisfactory 3D rendering quality.

The works already devoted to the quality assessment of 3D images (Benoit, 2008), (Kilner, 2009) does not suit our research goals focalised rather on the impact of inaccurate positioning on the rendering quality. For that we propose two approaches helping in the determination of the positioning accuracy. The first one is based on visual assessment tests of 3D rendering quality by human

observers. The second one is based on human visual acuity.

This paper is organized as follows: in Section 2, the positioning accuracy problem is posed after recalling the shooting/viewing geometrical process of parallel and decentring configuration for auto-stereoscopic rendering and deriving a simulation scheme of this process. In Section 3, the visual observation based method of rendering quality assessment is presented with the used tools and the obtained simulation results. In Section 4, the visual acuity based method is presented with the obtained results. We finish this work with some conclusions.

2 3D IMAGES SHOOTING / VIEWING GEOMETRICAL PROCESS

The Shooting/Viewing geometric process model consists in some geometric transformations from the capturing space to the rendering one. Thus, three groups of parameters can be defined: a rendering parameters group imposed by the auto-stereoscopic display geometry, a second group defining the geometric structure of the 3D camera model for capturing the scene, and a third one controlling the distortions that affect the 3D rendering. Knowing the parameters of these three groups and the relations between them, one can define a capturing configuration satisfying both parameters imposed by the visualization device and those of the wished distortions.

Thereafter, one recalls succinctly the different parts of this geometric process and the associated parameters (Prévoteau, 2010). In a first part, a multi-view rendering geometry of auto-stereoscopic display device is presented with the viewing parameters definition. Then, the shooting geometry of parallel and decentred configuration is presented defining the capture parameters. After that, relations between capturing and viewing parameters are given to define the distortion controlling parameters.

2.1 Multi-view Rendering Geometry

The considered display device is an auto-stereoscopic screen as depicted in (Figure 1), where H and W represent respectively the height and the width of the device.

To perceive the 3D rendering, the observers should be at a preferential positions imposed by the screen and determined by a viewing distance d, a

lateral distance o_i and a vertical distance δ_o corresponding to a vertical elevation of the observer's eyes. Let b be the human binocular gap. A viewing frame $r = (C_r, x, y, z)$ is associated to the device in its centre C_r for expressing viewing geometry.
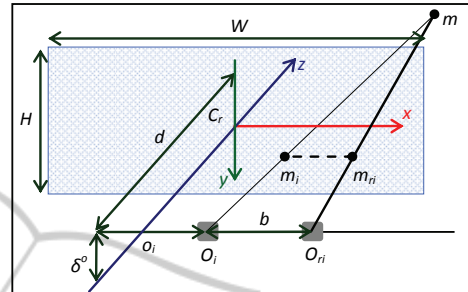
Figure 1: Viewing Geometry.

2.2 Shooting Geometry

The geometry of a parallel multi view shooting with decentred image sensors configuration is presented in (Figure 2).

a- Perspective view

b- Front view

c- Top view
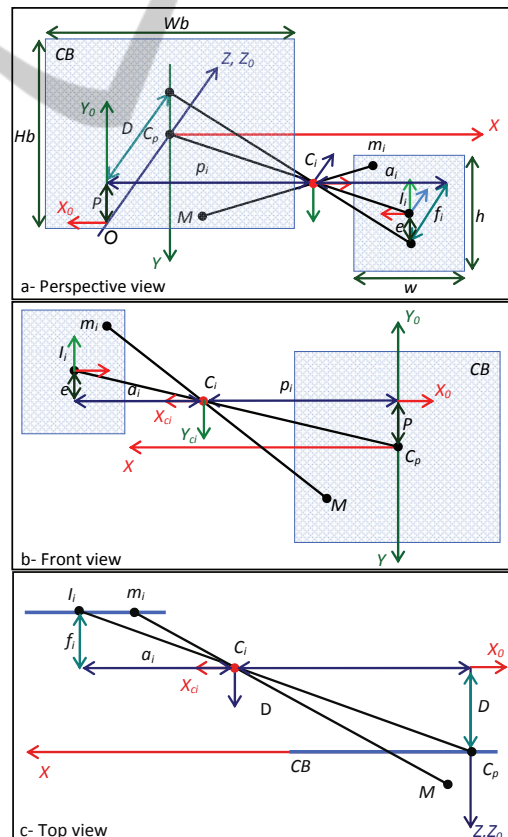
Figure 2: Shooting Geometry.

The shooting system is composed of n sensor/lens pairs. The lenses are represented by their optical centers C_i and the image sensors by their centers I_i and their dimensions $w \times h$. The optical centers are aligned and uniformly distanced by an inter-optical distance B along a parallel line to the scene plane CB having dimensions $Wb \times Hb$. This scene plane is situated at a convergence distance D from the line of optical centers. This line is elevated by a vertical distance P regarding to the scene plane centre C_p. Each optical centre C_i is defined by its lateral position p_i. Note that, these image planes are coplanar and parallel to CB plane and they are also distant by a focal length f to the optical centers line. In addition, each image plane is decentred by a lateral distance a_i and a vertical distance e regarding to the correspondent optical centre C_i. A frame $R = (C_p, X, Y, Z)$ is positioned at a chosen convergence centre C_p associated to the scene.

2.3 Transformation Parameters

The transition from the shooting space to the viewing one is expressed by the transformation between the captured point homogenous coordinates $M (X, Y, Z, 1)_R$ and those of the perceived point $m (x, y, z, 1)$ (Prévoteau, 2010):

$$\alpha \begin{bmatrix} x \\ y \\ z \\ 1 \end{bmatrix} = \begin{bmatrix} k \begin{vmatrix} \mu & & \gamma \\ & \rho\mu & \delta \\ & & 1 \end{vmatrix} & 0 \\ & & 0 \\ & & 0 \\ 0 & 0 & \frac{k(\varepsilon-1)}{d} & \varepsilon \end{bmatrix} \begin{bmatrix} X \\ Y \\ Z \\ 1 \end{bmatrix} \quad (1)$$

Where the transformation parameters quantifying independent distortion effects are defined as follows: $k = \dfrac{d}{D}$ is the global enlargement factor, $\varepsilon = \dfrac{b}{B} \dfrac{Wb}{W}$ controls the nonlinearity of depth distortion according to the global reduction rate $\alpha = \varepsilon + k(\varepsilon - 1)\dfrac{Z}{d}$, $\mu = \dfrac{b}{kB}$ controls the relative enlargement width/depth rate, $\rho = \dfrac{Wb}{Hb}\dfrac{H}{W}$ controls the relative enlargement height/width rate. $\gamma = \dfrac{p_i b - o_i B}{d \, B}$ controls the horizontal clipping rate and $\delta = \dfrac{\delta^o B - P b \rho}{d \, B}$ controls vertical clipping rate.

2.4 Specification of Multi-view Shooting Layout

Knowing the viewing, capturing and distortion parameters presented previously, one can specify a capturing layout satisfying the transformations and taking into account both the parameters imposed by the display device (Figure 2) and the parameters of the desired distortion $k, \varepsilon, \mu, \rho, \gamma$ and δ. Then, the geometrical parameters of the specified capture layout are pulled and expressed as follows:

$$W_b = \frac{W \varepsilon}{k \mu}, \quad H_b = \frac{H \varepsilon}{k \rho \mu}$$

$$w = \frac{W_b f}{D} = \frac{W f \varepsilon}{\mu d}, \quad h = \frac{H_b f}{D} = \frac{H f \varepsilon}{\mu \rho d}$$

$$D = \frac{d}{k}, \quad P = \frac{\delta^o - \delta d}{k \rho \mu}, \quad p_i = \frac{o_i + \gamma d}{k \mu} \quad (2)$$

$$a_i = \frac{p_i f}{D} = \frac{f (o_i + \gamma d)}{\mu d}$$

$$e = \frac{P f}{D} = \frac{f (\delta^o - \delta d)}{\mu \rho d}, \quad f = \frac{D F}{D + F}$$

The last relation of (2) is pulled from Descartes relation: $\dfrac{1}{f} = \dfrac{1}{D} + \dfrac{1}{F}$ and makes autofocus in order to obtain a sharp image on each point of view, where F is the lens focal.

Note that to obtain a perfect 3D rendering without distortions, it is sufficient to choose the distortion parameters as follows: $\varepsilon = 1$, $\mu = 1$, $\rho = 1$, $\gamma = 0$ and $\delta = 0$.

Based on this analysis some industrial applications such as 3D-CAM1 and 3D-CAM2 prototypes (Figure 3) were developed by our partner 3DTV-Solutions Society. These prototypes are able to capture images of eight points of view simultaneously and which can be displayed, after interlacing, on an auto-stereoscopic screen in real-time. Note however that these prototypes are designed only for static and quasi-static scenes presenting one constant and known convergence distance for each prototype.

Figure 3: 3D-CAM1 and 3D-CAM2 prototypes.

2.5 The Simulation Scheme

A simulation scheme reproducing the global shooting/rendering geometrical process is given in (Figure 4). It exploits a perspective projection model based on the parameters defined above in the case of static scenes by assuming the convergence distance of the camera to be equal to the real distance of the scene.
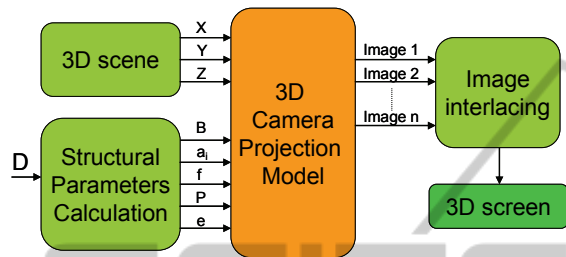
Figure 4: Simulation scheme of the production process

The obtained simulation results under Matlab/Simulink environment are presented in (Figure 5). The delivered 3D images and 3D videos are visualized on an auto-stereoscopic screen showing an optimal 3D rendering. This validates viewing, projection and shooting geometry.
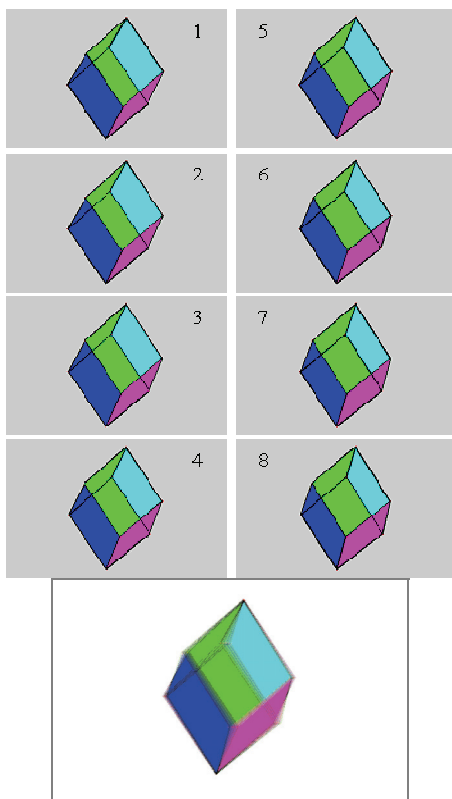
Figure 5: The eight points of view and resultant 3D image.

2.6 Positioning Accuracy Problem of the Shooting Parameters

To obtain an optimal 3D rendering, it is necessary to ensure that the images of the different points of view are coherent between them. Theoretically, an optimal coherence of these images depends on the correspondence of each pixel of each image to a precise position in the 3D image obtained after interlacing. In practice, it is not possible to achieve a zero positioning error of image sensors, so a positioning error threshold of the shooting parameters should be determined. Thus, the image sensors should be positioned in a precision of a fraction of pixel near. This pixel fraction will penalize the quality of the 3D rendering as far as it will be significant. Ever since, the problem is how to specify a positioning accuracy that is sufficient to provide a satisfactory 3D rendering quality practically achievable?

To attempt an answer to this problem we adopt two different approaches. The first one is based on a visual appreciation to determine the positioning error threshold. Moreover, this method is based on some quantization tools using error images. It will be presented in the next section. The second method is based on the acquired expert knowledge on human visual acuity. The latter represents a reference error back-propagated through the geometrical production process in order to specify a positioning accuracy of the image sensors to ensure a satisfactory perceived rendering. This method will be presented in Section 4.

3 VISUAL OBSERVATION BASED METHOD

This method consists in soiling the various shooting geometrical parameters by different error values. The resulting 3D images are compared visually to a reference 3D image obtained under ideal conditions where the parameters of shooting are calculated theoretically. The threshold of the error affecting each geometrical parameter is fixed when the lack of 3D rendering quality begins to be discernible by the observers. Moreover, to get a quantitative appreciation of the geometrical parameters' error extent and their repercussion on the 3D rendering quality, an error image is defined and then quantified. The quantization of these error images will serve to compare the different accuracies in terms of numerical quantities what constitutes a valuable tool in our study. The image error quantifi-

cation consists in counting the number of the coloured pixels to define an absolute error. A relative error is also defined by dividing the absolute error by the number of the coloured pixels of the reference image. An index of quality is also defined to express directly the rendering quality.

3.1 Error Images

An error image is an image produced by the subtraction of two images $im_{err} = im_{ref} - im$. In our case it allows the comparison of an image affected by a positioning error of the image sensors to a reference image obtained by a perfect positioning of them (Figure 6):
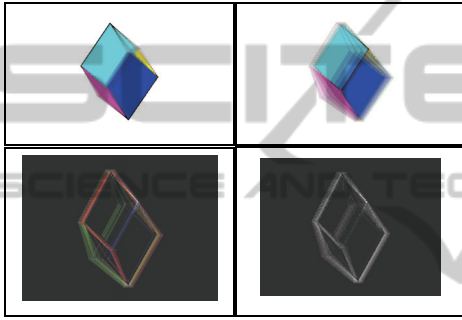
Figure 6: Reference, current and error images.

3.2 Error Images Quantization

To quantify the error images, we adopt methods based on counting the number of coloured pixels in the images. To avoid redundant counting of pixels, RGB images are converted to greyscale images giving one matrix for each image (Figure 6). The absolute error N_{abs} is obtained by counting the coloured pixels in the error image compared to an image obtained with not erroneous parameters. The relative error N_{relat} is the ratio between the number of coloured pixels in the current image error N_{abs} and the number of coloured pixels in the reference image N_{ref} at the same instant. We define it as follows:

$$N_{relat} = \frac{N_{abs}}{N_{ref}} \quad (3)$$

This error can be expressed also in percentage $N_{relat}\% = N_{relat} \times 100$. We also adopt the complement to 1 of the relative error representing the image quality:

$$Q = 1 - \frac{N_{abs}}{N_{ref}} \quad (4)$$

Thus the error is smaller when Q is closer to 1.

3.3 Repercussion of the Shooting Parameters Error on the Rendering Quality

In this section we are interested in the repercussion of some shooting parameters positioning error i.e. the inter-optical distance B, the lateral decentring a_i and the focal length f on the 3D rendering quality. The obtained 3D images for different positioning errors are displayed on an auto-stereoscopic screen and assessed visually. The corresponding quantified errors are grouped in a table to compare the impact of the different positioning errors on the 3D rendering quality.

3.3.1 Error on Inter-optical Distance

For the different positioning errors committed on the inter-optical distance B, visual assessment and quantification of the corresponding error images are summarized in the Table 1. The retained value of the accuracy threshold corresponds to the satisfactory visual assessment where $\Delta B = 40.6$ μm.

Table 1: Image quantization and visual assessment.

Error B (%)	0.5	0.1	0.05	0.01
ΔB (μm)	406.3	81.2	**40.6**	8.12
$N_{relat\%}$ (%)	0.8933	0.1790	0.1180	0.0075
$Quality(Q)$	0.9911	0.9982	0.9988	0.9999
Visual Assessment	Bad	Slightly bad	**Satis-factory**	Perfect

3.3.2 Error on Lateral Decentring

In the same way, for the different positioning errors committed on the lateral decentring a_i, visual assessment and quantification of the corresponding error images are summarized in the Table 2.

Table 2: Image quantization and visual assessment.

Error a_i (%)	0.5	0.1	0.01	0.001
Δa_i (μm)	2 - 8	0.4-1.6	**0.04-0.16**	-
$N_{relat\%}$ (%)	0.9146	0.1934	0.0377	0
$Quality (Q)$	0.9909	0.9981	0.9996	1
Visual Assessment	Bad	Slightly bad	**Satis-factory**	Perfect

The retained value of the accuracy threshold corresponds to the satisfactory visual assessment where Δa_i vary between 0.04 and 0.16 μm according to i leading to an average of $\Delta a = 0.1$ μm.

3.3.3 Error on Focal Length

Again, for the different positioning errors committed

on the focal length *f*, visual assessment and quantification of the corresponding error images are summarized in the Table 3. The retained value of the accuracy threshold of *f* corresponds to the satisfactory visual assessment where $\Delta f = 1.72$ μm.

Table 3: Image quantization and visual assessment.

Error f (%)	1	0.1	0.01	0.001
Δf (μm)	172	17.2	**1.72**	0.172
$N_{relat\%}$ (%)	1.0633	0.2332	0.0302	0
$Quality(Q)$	0.9894	0.9977	0.9997	1
Visual Assessment	Bad	Slightly bad	**Satis-factory**	Perfect

The precisions retained in these three cases are fixed by considering the parameters separately. By considering them together with the retained accuracies, the visual observation assessed the obtained 3D rendering as satisfactory and the quantification of the error image gives the following values: $N_{ref} = 2288529$ p, $N_{abs} = 2871$ p, $N_{relat} = 0.0013$, $N_{relat\%} = 0.1255$ %, $Q = 0.9987$.

Remark: This method requires significant investment of time to perform sufficient tests to properly determine the threshold positioning error of each shooting parameter to ensure a satisfactory 3D rendering. In this study we have considered a single scene, also plenty of scenes with other conditions of shooting should be considered to refine more the values of positioning accuracies sought.

4 VISUAL ACUITY BASED METHOD

The quantification of the error images were used to compare the different accuracies and to establish thresholds of acceptable error by using visual assessment of the obtained 3D images, therefore, this approach still relatively subjective.

We propose in this section to establish an objective relation between different degrees of human visual acuity and the positioning accuracy of the camera parameters to get a quality 3D rendering. From the precision of human vision (visual acuity), we'll go back up the production chain of the 3D perception as far as the shooting parameters positioning accuracy, through the resolution of both a given auto-stereoscopic screen and given image sensors (Figure 7).
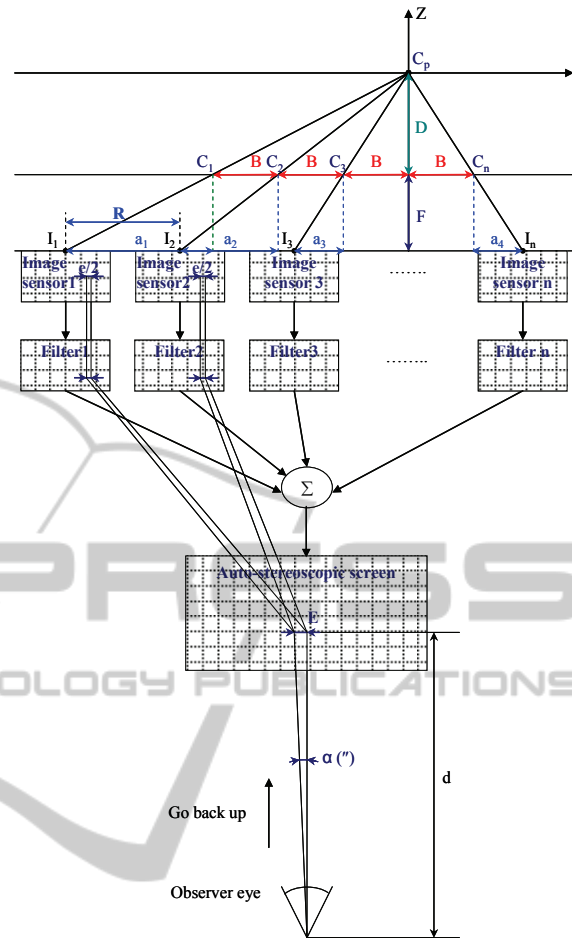
Figure 7: 3D perception scheme of multi-view production.

4.1 Objective Relation: Visual Acuity / Sensors Positioning Accuracy

The idea is to define a positioning error of image sensors small enough so that a human eye with good visual acuity is unable to detect it on the 3D image displayed on a given auto-stereoscopic screen.

Indeed, the relation between the visual acuity angle *α* and the gap *E* which can be detected on a screen surface situated at a viewing distance *d* is expressed as follows:

$$E = 2*d*tang(\alpha/2) \qquad (5)$$

This gap is equal to a proportion of the pitch of the screen defined by:

$$\lambda = E / pitch\_scr \qquad (6)$$

A given pixel of the image displayed on the screen corresponds to a well-defined pixel of an image captured by one of the *n* image sensors of the camera. Thus, a pixel in one of these sensors should not undergo a positioning error greater than:

$$e = \lambda * pitch\_sens \qquad (7)$$

From (5), (6) and (7) we obtain the relation between the acuity angle α and the positioning error of the sensors:

$$e = 2*d*tang(\alpha/2)*pitch\_sens / pitch\_scr \qquad (8)$$

At this stage an objective relation between the accuracy of sensors positioning and 3D rendering quality expressed by the visual acuity of the observer is derived.

4.2 Positioning Accuracy of the Different Degree of Freedom

The questions to be answered here are: how to share out the error e? And how to determine the positioning accuracy of the different degree of freedom: the inter-optical distance B, the lateral decentring a_i of the sensors and the focal length?

In 3D perception, each observer eye observes a different picture of the scene. At the capturing space level, these two images stemming from two adjacent sensors are separated by a distance R.

The positioning error e defines the error committed on the positioning of each pair of sensors separated by the inter-sensor distance R defined as follows:

$$R = B + (a_i - a_{i-1}) \qquad (9)$$

The error ΔR must not exceed the value of e:

$$\Delta R \leq |e| \qquad (10)$$

With

$$\Delta R = \Delta B + \Delta a_i + \Delta a_{i-1} \qquad (11)$$

This error can be written as follows:

$$\Delta R = \frac{B}{R}\Delta R + \frac{|a_i - a_{i-1}|}{R}\Delta R \qquad (12)$$

With

$$\Delta B = \frac{B}{R}\Delta R \quad \text{and} \quad \Delta a_i + \Delta a_{i-1} = \frac{|a_i - a_{i-1}|}{R}\Delta R \qquad (13)$$

Note that a_i-a_{i-1} is constant for all i, since R and B have the same value for all pairs of adjacent sensors at a given time. One can note that the quasi-totality of the error should be endorsed to the error on B and a tiny part is authorized as error on the lateral decentring a_i. This implies a maximum permissible error on a_i-a_{i-1} of the order of $10^{-3}*\Delta R$.

This error is evenly divided on both sensors lateral decentring, so we obtain a common value of the absolute error:

$$\Delta a = \frac{\Delta(a_i - a_{i-1})}{2} \qquad (14)$$

Concerning the error on the focal length it is deduced from the following relations:

$$a_i = \frac{p_i(t)}{D(t)} * f = i * \frac{B(t)}{D(t)} * f \qquad (15)$$

$$\frac{B(t)}{D(t)} = \frac{b}{d} = cste \qquad (16)$$

$$a_i = i * \frac{b}{d} * f \qquad (17)$$

$$f = \frac{d}{i*b} * a_i \qquad (18)$$

The ratio of errors is maintained for a coherent two-dimensional autofocus (lateral and depth), in addition, the maximum permissible error on the lateral decentring is the same for all points of view:

$$\Delta f = \frac{d}{b} * \Delta a \qquad (19)$$

The error on f is thus of the order of $d/b*10^{-3}*\Delta R$.

4.3 Validation using the Visual Observation based Method

We will use the tools provided in the method based on visual observation to evaluate the practical validity and relevance of this second method.

We perform a test using a 30" screen whose pitch is 0.5025 mm and minimum viewing distance is $d = 2$ m. The pitch of the sensors is 3.2 μm and the considered visual acuity is $\alpha = 1$'. After calculation, we obtain the following values: $E = 0.5818$ mm, $\lambda = 1.1578$, $\Delta R = 3.7049$ μm, $\Delta B = 3.6911$ μm, $\Delta a = 0.0097$ μm, $\Delta f = 0.2985$ μm.

Now by visual assessment, the 3D rendering for acuity of 1' is evaluated as **"perfect"** and the image error's quantization gives the values : $N_{ref} = 979875$ p, $N_{abs} = 0$ p, $N_{relat} = 0$, $N_{relat\%} = 0$ % and $\boldsymbol{Q = 1}$.

For a 24" screen with a pitch of 0.27 mm and a viewing distance of 2 m, we obtain the values: $E = 0.5818$ mm, $\lambda = 2.1548$, $\Delta R = 6.8954$ μm, $\Delta B = 6.8698$ μm, $\Delta a = 0.0168$ μm, $\Delta f = 0.5179$ μm.

The 3D rendering is visually assessed as **"perfect"** and the quantified image error values are: $N_{ref} = 2294208$ pixels, $N_{abs} = 287$pixels, $N_{relat} = 1.2510*10^{-4}$, $N_{relat\%} = 0.0125$ % and $\boldsymbol{Q = 0.9999}$.

This method is considered as severe regarding to the applicability of the obtained results. However, a compromise can be envisaged for a practical solution by choosing a reasonable precision for Δa and ΔB. Δf can be then deducted by calculation.

For example if we choose a precision of 0.1μm for Δa, the accuracy of the other parameters is: $\Delta R =$

40.816 μm, $\Delta B = 40.6653$ μm, $\Delta f = 3.0769$ μm.

The results obtained by quantifying the error images are: $N_{ref} = 2294208$ pixels, $N_{abs} = 783$ pixels, $N_{relat} = 3.4129 * 10^{-4}$, $N_{relat\%} = 0.0341$ % and **Q=0.9997** and the quality of the 3D rendering is visually assessed as **satisfactory**.

5 CONCLUSIONS

In this paper, after validating experimentally the global shooting/viewing geometrical process for auto-stereoscopic visualization, a visual observation method has been proposed to assess the rendering quality depending on the positioning accuracy of the image sensors. Hence, a suitable accuracy is fixed when 3D rendering is assessed to be satisfactory. This is done with quantifying the error images to compare the positioning error impacts of the different structural shooting parameters.

In this method, the error images express the inconsistency of the different viewpoint images. Hence, with their quantification, a relation between the images inconsistency and the visual assessment can be achieved.

The quantification of error images and its relation regarding to the visual assessment of the rendering quality can constitute a basis for learning after a sufficient number of tests. This basis will exempt us from the visual assessment of the 3D image quality and it will be sufficient to only use the quantification of the error image including the relative error.

The second proposed method provides an objective relation between the visual acuity expressing the quality and the positioning accuracy of shooting parameters. This relation can be used to specify any implying parameter (*e*, *d*, pitch of the sensor pixels or pitch of the screen pixels) by taking into account the other ones.

ACKNOWLEDGEMENTS

REFERENCES

Ali-Bey M., Manamanni N., Moughamir S., 2010, 'Dynamic Adaptation of Multi View Camera Structure', *3DTV-Conference: The True Vision - Capture, Transmission and Display of 3D Video (3DTV-CON'10),* Tampere, Finland.

Ali-Bey M, Moughamir S, Manamanni N, 2010, 'Towards Structurally Adaptive Multi-View Shooting System', *18th Mediterranean Conference on Control and Automation (MED)*, Marrakesh, Morocco.

Benoit A., Le Callet P., Campisi P., Cousseau R., 2008, 'Quality Assessment of Stereoscopic Images', *Hindawi, EURASIP Journal on Image and Video Processing*. doi:10.1155/2008/659024.

Blach R., Bues M., Hochstrate J., Springer J., Fröhlich B., 2005, 'Experiences with multi-viewer stereo displays based on lc-shutters and polarization', *In Proceedings of IEEE VR Workshop: Emerging Display Technologies.*

Dodgson N. A., 2002, 'Analysis of the viewing zone of multi-view autostereoscopic displays', *In Stereoscopic Displays and Virtual Reality Systems IX*, vol. 4660 of Proceedings of SPIE, pp. 254–265.

Dubois E., 2001, 'A projection method to generate anaglyph stereo images' *In Proc. IEEE Int. Conf. Acoustics, Speech, and Signal Processing (ICASSP '01)*, vol. 3, pp. 1661–1664, IEEE Computer Society Press.

Graham J., Delman L., Nicolas H., David E., 2001, 'Controlling perceived depth in stereoscopic images', *In Proc. SPIE Stereoscopic Displays and Virtual Reality Systems VIII*, 4297:42-53, June.

Güdükbay U., Yilmaz T., 2002, 'Stereoscopic view-dependent visualization of terrain height fields', *IEEE Trans. on Visualization and Computer Graphics*, vol. 8, no. 4, pp. 330–345.

Kilner J., Starck J., Guillemaut J. Y., Hilton A., 2009, 'Objective quality assessment in free-viewpoint video production', *Signal Processing: Image Communication*, vol. 24, no. 1-2, pp. 3-16.

Meesters L. M. J., Wijnand A. IJsselsteijn, Pieter J. H. Seuntiëns, 2004, 'A Survey of Perceptual Evaluations and Requirements of Three-Dimensional TV', *IEEE Trans. on Circuits and Systems for Video Technology*, vol. 14, no. 3, pp. 381 – 391.

Müller K., Smolic A., Dix K., Merkle P., Kauff P., Wiegand T., 2008, 'View synthesis for advanced 3D video systems', *Hindawi Publishing Corporation, EURASIP Journal on Image and Video Processing.*

Perlin K., Paxia S., Kollin J. S., 2000, 'An autostereoscopic display', *In Proceedings of the 27th ACM Annual Conference on Computer Graphics (SIGGRAPH '00)*, vol. 33, pp. 319–326.

Prévoteau J., Chalençon-Piotin S., Debons D., Lucas L., Remion Y., 2010, 'Multi-view shooting geometry for multiscopic rendering with controlled distortion', *Hindawi, Int. Journal of Digital Multimedia Broadcasting (IJDMB), Advances in 3DTV: Theory and Practice.*

Sanders W., McAllister D. F., 2003, 'Producing anaglyphs from synthetic images', *In Stereoscopic Displays and Virtual Reality Systems X*, vol. 5006 of Proceedings of SPIE, pp. 348–358.